JACS
JOURNAL OF THE AMERICAN CHEMICAL SOCIETY

COMMUNICATION

pubs.acs.org/JACS

Very Large, Soluble Endohedral Fullerenes in the Series La_2C_{90} to La_2C_{138}: Isolation and Crystallographic Characterization of $La_2@D_5(450)$-C_{100}

Christine M. Beavers,[†] Hongxiao Jin,[‡] Hua Yang,[‡] Zhimin Wang,[‡] Xinqing Wang,[‡] Hongliang Ge,[‡] Ziyang Liu,[*,‡] Brandon Q. Mercado,[§] Marilyn M. Olmstead,[*,§] and Alan L. Balch[*,§]

[†]Advanced Light Source, Lawrence Berkeley National Laboratory, One Cyclotron Road, Berkeley, California 94720, United States

[‡]College of Materials Science and Engineering, China Jiliang University, Hangzhou 310027, China

[§]Department of Chemistry, University of California, One Shields Avenue, Davis, California 95616, United States

Supporting Information

ABSTRACT: An extensive series of soluble dilanthanum endohedral fullerenes that extends from La_2C_{90} to La_2C_{138} has been discovered. The most abundant of these, the nanotubular $La_2@D_5(450)$-C_{100}, has been isolated in pure form and characterized by single-crystal X-ray diffraction.

The formation and characterization of fullerenes and endohedral fullerenes with large numbers of carbon atoms in the cage represent a seemingly endless frontier. However, as the carbon cage size expands, so does the number of possible isomers for a particular cage size.[1] Hence, identification of the structures of large fullerene cages can be challenging. For empty cages, the isolated pentagon rule (IPR), which is based on avoiding direct pentagon−pentagon contact, provides a guide for limiting the structural possibilities.[1] Empty-cage fullerenes as large as C_{250} have been extracted from arc-generated carbon soot and identified by mass spectrometry.[2] Reactive extraction of similar soot with an *o*-quinidimethane precursor yielded addition products of fullerenes with even larger sizes that ranged from C_{60} to C_{418}.[3] The largest empty-cage fullerenes that have been obtained in pure form and crystallographically characterized are three isomers of C_{90}: the unsymmetrical isomers $C_1(30)$-C_{90} and $C_1(32)$-C_{90}[4] and nanotubular $D_{5h}(1)$-C_{90}.[5]

Many large carbon cages are found with endohedral fullerenes. For example, $La@C_{82}$ and $La_2@C_{80}$ are among the most extensively studied endohedral fullerenes.[6] In addition to soluble $La@C_{82}$ and $La_2@C_{80}$, Whetten and co-workers found mass spectroscopic evidence for the presence of insoluble dilanthanum endohedrals with compositions ranging from La_2C_{74} to La_2C_{100} and a second series of insoluble trilanthanum endohedrals with compositions La_3C_{102} to La_3C_{126}.[7] Additionally, there is a brief mention of a soluble species, LaC_{106}.[8] Yang and Dunsch prepared and isolated pure samples of two isomers of Dy_2C_{94} as well as Dy_2C_{98} and Dy_2C_{100}.[9] An extensive series of endohedral fullerenes containing two gadolinium atoms with apparent cage sizes running from C_{90} to C_{124} have been observed.[10] Currently, the largest fullerene cage that has been crystallographically identified is $Sm_2@D_{3d}(822)$-C_{104}, which has a nanotubular shape.[11] Endohedral fullerenes containing the M_3N unit, such as $Sc_3N@I_h$-C_{80}, can be obtained in unusually high yields for molecules of this class,[12] and one might expect large cages to be encountered in this class of molecules. The largest of the endohedrals of this type are $La_3N@C_{88}$, $La_3N@C_{92}$, $La_3N@C_{96}$, and $La_3N@C_{104}$, of which all but the last have been isolated and characterized by UV−vis spectroscopy and cyclic voltammetry.[13]

Probably because of the iconic nature of a cage of 100 carbon atoms, there have been several predictions of the preferred cage isomers for M_2C_{100}. After isolating Dy_2C_{100}, Yang and Dunsch suggested that the effect of charge transfer between the encapsulated metal atoms and the fullerene cage could be ignored and that the most stable empty-cage isomers of C_{100}, namely, $D_2(449)$-C_{100}, $C_2(10)$-C_{100}, $C_1(140)$-C_{100}, $C_1(425)$-C_{100}, $C_1(426)$-C_{100}, and $C_2(442)$-C_{100}, were the most likely hosts.[9] In contrast, Valencia, Rodríguez-Fortea, and Poblet emphasized the role of electron transfer between the metal atoms and the cages and found that the $D_5(450)$-C_{100} cage was an unusually promising candidate for encapsulating a unit such as Sc_3N or La_2 that could transfer six electrons to the cage.[14] Finally, Yang, Zhao, and Nagase considered the possibility that Dy_2C_{100} might involve a non-IPR cage and performed computations on 24 755 possible isomers of the C_{100} cage.[15] They concluded that the IPR-obeying $D_5(450)$-C_{100} cage would be the most likely host. However, there is an alternative possibility for the structure of M_2C_{100} that involves the presence of a carbide unit within the cage. Several such metal carbides have been identified. For example, Gd_2C_{94} has been shown to be $Gd_2(\mu_2\text{-}C_2)@D_3(85)$-$C_{92}$[9], and Sc_2C_{82} has been identified as $Sc_2(\mu_2\text{-}C_2)@C_{2v}(5)$-$C_{80}$.[16] Here we report the detection of a series of soluble endohedral fullerenes from La_2C_{90} to La_2C_{138} and the isolation and crystallographic characterization of $La_2@D_5(450)$-C_{100}.

To obtain $La_2@D_5(450)$-C_{100}, a graphite rod filled with La_2O_3 and graphite powder was vaporized in an electric arc by the classic Krätschmer−Hoffmann method of fullerene formation. The soluble material obtained by extraction of the soot with chlorobenzene contained a variety of dilanthanum endohedrals from La_2C_{92} to La_2C_{134}, as the data in Figure 1 show. Extensive chromatographic separations (as documented in the Supporting Information) led to the isolation of $La_2@D_5(450)$-C_{100}. Figure 2 shows the chromatograms and laser-desorption ionization time-of-flight (LDI-TOF) mass spectra of the purified sample of $La_2@D_5(450)$-C_{100}.

Received: July 28, 2011
Published: August 24, 2011

dx.doi.org/10.1021/ja207090e | *J. Am. Chem. Soc.* 2011, 133, 15338–15341

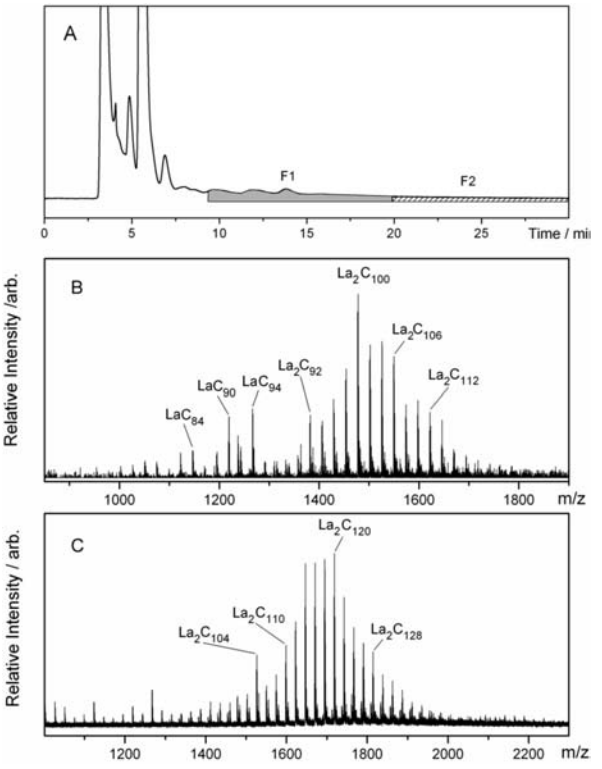

Figure 1. (A) Chromatogram from the initial HPLC of the extract on a Buckyprep-M column (mobile phase, chlorobenzene; flow rate, 4.0 mL/min; detection wavelength, 450 nm). (B) LDI-TOF mass spectrum obtained from fraction F1. (C) LDI-TOF mass spectrum obtained from fraction F2.

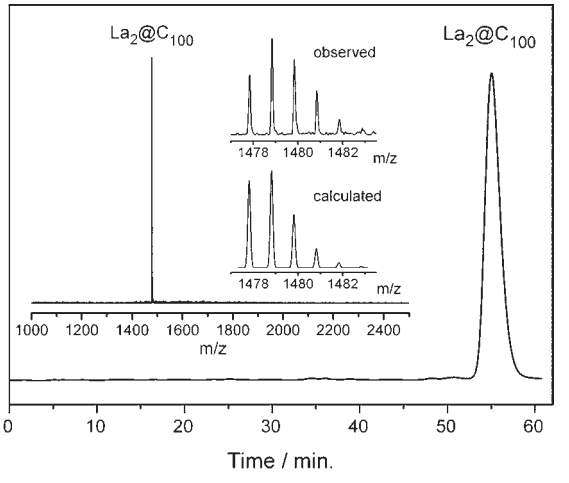

Figure 2. HPLC chromatogram of purified $La_2@D_5(450)$-C_{100} on a Buckyprep-M column with toluene as the eluent (HPLC conditions: flow rate, 4.5 mL/min; detection wavelength, 450 nm). The inset shows the LDI-TOF mass spectrum and expansions of the observed and calculated isotope distributions for $La_2@C_{100}$.

The UV−vis−NIR spectrum of this compound is shown in Figure 3. The spectrum differs from that reported earlier for Dy_2C_{100}, which has a low-energy absorption at ~1060 nm.[7] Consequently, these two compounds may involve different cages, or the presence of the paramagnetic dysprosium may influence the electronic spectrum.

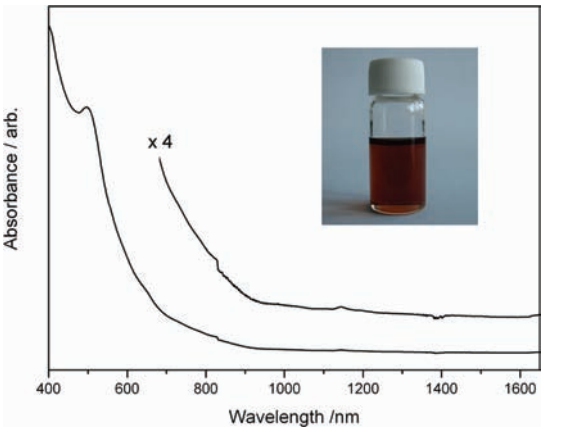

Figure 3. UV−vis−NIR absorption spectrum of purified $La_2@D_5$-(450)-C_{100} dissolved in carbon disulfide. The inset shows a picture of a vial containing a CS_2 solution of $La_2@D_5(450)$-C_{100}.

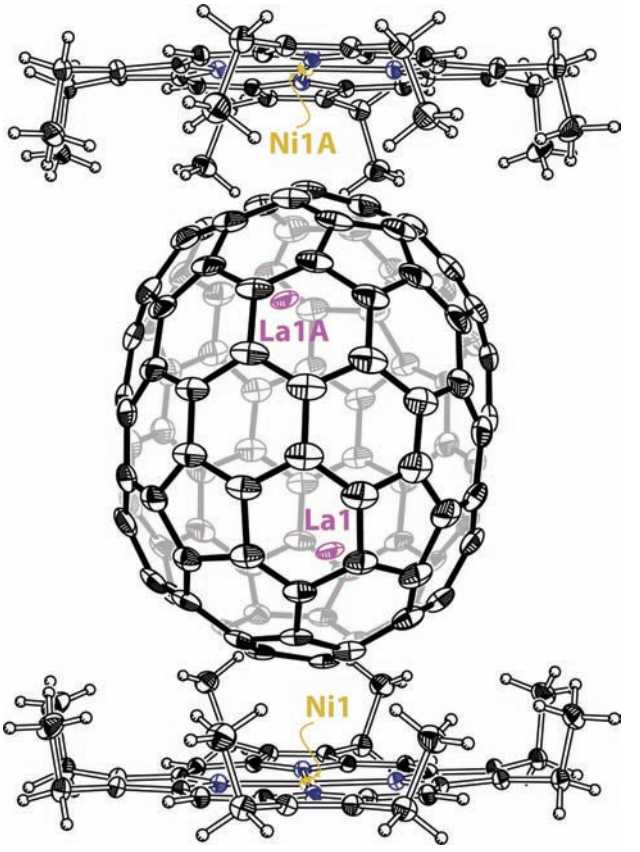

Figure 4. Drawing showing how the $La_2@D_5(450)$-C_{100} molecule is suspended between two molecules of Ni^{II}(OEP) in $La_2@D_5(450)$-$C_{100}\cdot 2Ni^{II}(OEP)\cdot 2$(toluene). This view shows only one orientation of the C_{100} cage and only the major La site [0.6891(13) site occupancy] along with the symmetry-generated La1A site. Solvate molecules have been omitted for clarity.

Black crystals of $La_2@D_5(450)$-$C_{100}\cdot 2Ni^{II}(OEP)\cdot 2$(toluene) (OEP = 2,3,7,8,12,13,17,18-octaethylporphin dianion) suitable for X-ray diffraction were obtained by slow diffusion of a toluene solution of $La_2@D_5(450)$-C_{100} into a toluene solution of Ni^{II}-(OEP). The structure of $La_2@D_5(450)$-C_{100} and the two Ni(OEP)

dx.doi.org/10.1021/ja207090e |J. Am. Chem. Soc. 2011, 133, 15338–15341

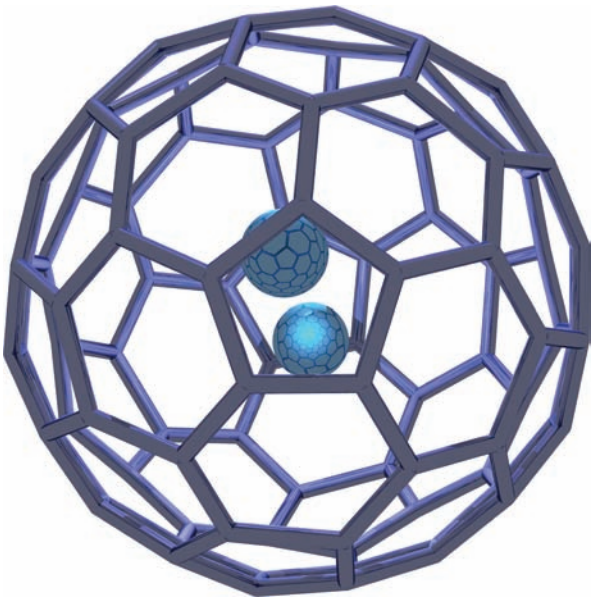

Figure 5. Drawing of the $La_2@D_5(450)$-C_{100} molecule with the fivefold axis perpendicular to the picture plane.

molecules that surround it are shown in Figure 4.[17] Figure 5 shows a view of the $La_2@D_5(450)$-C_{100} molecule looking down the fivefold axis.

The structure does suffer from disorder. The fullerene cage is chiral but occupies a centrosymmetric site in the crystal. There are four equally populated sites for the fullerene cage, two for each enantiomer. There are four sites occupied by the lanthanum ion with fractional occupancies of 0.6891(13), 0.1242(16), 0.1072(10), and 0.0794(14).

Several features of the structure are noteworthy. The endohedral fullerene is clearly a conventional dimetallofullerene and not a carbide. The carbon cage has a nanotubular shape similar to those of the large carbon cages in $Sm_2@D_{3d}(822)$-C_{104}[11] and $D_{5h}(1)$-C_{90}.[5] The centroid-to-centroid distance between pentagons on the major axis is 10.083 Å. There are five perpendicular twofold axes, all of which bisect 6:6 ring junctions, and their average centroid-to-centroid distance is 8.024 Å. The cage structure is consistent with theoretical predictions indicating that the $D_5(450)$-C_{100} cage is best suited for encapsulating an $(M^{3+})_2$ unit.[14] This cage also provides maximal separation between the pentagons, which are the sites of negative charge localization in the fullerene anions.[18] Notably, the lanthanum ions are found in the curved poles of the cage where the pentagons are located. Additionally, the $D_5(450)$-C_{100} cage occupies a unique place as the final entry in the listing of fullerenes given by Fowler and Manolopoulous.[1]

Within the cage, the lanthanum ions are displaced slightly from the fivefold axis of the fullerene cage. They are widely separated because of the repulsion of the two cations, as seen in other lanthanum-containing endohedrals.[19] The distance between La1 and La1A is 5.7441(4) Å. For comparison, the theoretical Dy---Dy separation computed for $Dy_2@D_5(450)$-C_{100} is 5.624 Å.[9]

In the crystal, each molecule of $La_2@D_5(450)$-C_{100} is surrounded by two molecules of Ni(OEP), as shown in Figure 4. Surprisingly, the $La_2@D_5(450)$-C_{100} molecule is suspended with its long axis perpendicular to the planes of the two porphyrins. This orientation places the most curved portion of the fullerene cage adjacent to the planar Ni(OEP) molecules. This arrangement differs from the situations in crystals of $Sm_2@D_{3d}(822)$-$C_{104}\cdot 2Ni(OEP)\cdot C_6H_5Cl$ and $D_{5h}(1)$-$C_{90}\cdot Ni^{II}(OEP)$, where these nanotubular fullerenes are oriented to place the two neighboring Ni(OEP) molecules near the less-curved interior portions of the carbon cage. In $La_2@D_5(450)$-$C_{100}\cdot 2Ni^{II}(OEP)\cdot 2(toluene)$, the Ni1---Ni1A separation across the fullerene cage is 15.8785(6) Å, while in centrosymmetric $Sm_2@D_{3d}(822)$-$C_{104}\cdot 2Ni(OEP)\cdot C_6H_5Cl$, the corresponding Ni---Ni separation [14.3850(13) Å] is smaller, despite the fact that the fullerene cage is a bit larger.

In summary, a series of large and soluble endohedral fullerenes that extends from La_2C_{90} to La_2C_{138} has been detected. The most abundant of these, $La_2@D_5(450)$-C_{100}, has been isolated and characterized by single-crystal X-ray diffraction.

■ ASSOCIATED CONTENT

Supporting Information. Preparative and separation information for $La_2@D_5(450)$-C_{100} and X-ray crystallographic data for $D_5(450)$-$La_2@C_{100}\cdot 2Ni^{II}(OEP)\cdot 2(toluene)$ (CIF). This material is available free of charge via the Internet at http://pubs.acs.org.

■ AUTHOR INFORMATION

Corresponding Author

zyliu@zju.edu.cn; mmolmstead@ucdavis.edu; albalch@ucdavis.edu

■ ACKNOWLEDGMENT

We thank the U.S. National Science Foundation (Grant CHE-1011760 to A.L.B. and M.M.O.), the U.S. Department of Education for a GAANN Fellowship to B.Q.M., the National Natural Science Foundation of China (20971108 to Z.L.), the Natural Science Foundation of Zhejiang Province of China (Y4090430 to Z.W.), and the State Key Laboratory of Superhard Materials in Jilin University (201105 to H.Y.) for support and Dr. Simon Teat for experimental assistance. The Advanced Light Source is supported by the Director, Office of Science, Office of Basic Energy Sciences, U.S. Department of Energy, under Contract DE-AC02-05CH11231.

■ REFERENCES

(1) Fowler, P. W.; Manolopoulous, D. E. *An Atlas of Fullerenes*; Clarendon: Oxford, U.K., 1995.

(2) Diederich, F.; Ettl, R.; Rubin, Y.; Whetten, R. L.; Beck, R.; Alvarez, M.; Anz, S.; Sensharma, D.; Wudl, F.; Khemani, K. C.; Koch, A. *Science* **1991**, *252*, 548–551.

(3) Beer, F.; Gügel, A.; Martin, K.; Räder, J.; Müllen, K. *J. Mater. Chem.* **1997**, *7*, 1327–1330.

(4) Yang, H.; Mercado, B. Q.; Jin, H.; Wang, Z.; Jiang, A.; Liu, Z.; Beavers, C. M.; Olmstead, M. M.; Balch, A. L. *Chem. Commun.* **2011**, *47*, 2068–2070.

(5) Yang, H.; Beavers, C. M.; Wang, Z.; Jiang, A.; Liu, Z.; Jin, H.; Mercado, B. Q.; Olmstead, M. M.; Balch, A. L. *Angew., Chem. Int. Ed.* **2010**, *49*, 886–890.

(6) (a) Sato, S.; Seki, S.; Honsho, Y.; Wang, L.; Nikawa, H.; Luo, G.; Lu, J.; Haranaka, M.; Tsuchiya, T.; Nagase, S.; Akasaka, T. *J. Am. Chem. Soc.* **2011**, *133*, 2766–2771. (b) Feng, L.; Slanina, Z.; Sato, S.; Yoza, K.; Tsuchiya, T.; Mizorogi, N.; Akasaka, T.; Nagase, S.; Martín, N.; Guldi, D. M. *Angew. Chem., Int. Ed.* **2011**, *50*, 5909–5912. (c) Johnson, R. D.; Devries, M. S.; Salem, J.; Bethune, D. S.; Yannoni, C. S. *Nature* **1992**, *355*, 239–240.

(7) Alvarez, M. M.; Gillan, E. G.; Holczer, K.; Kaner, R. B.; Min, K. S.; Whetten, R. L. *J. Phys. Chem.* **1991**, *95*, 10561–10563.
(8) Yeretzian, C.; Hansen, K.; Alvarez, M. M.; Min, K. S.; Gillan, E. G.; Holczer, K.; Kaner, R. B.; Whetten, R. L. *Chem. Phys. Lett.* **1992**, *196*, 337–342.
(9) Yang, S. F.; Dunsch, L. *Angew. Chem., Int. Ed.* **2006**, *45*, 1299–1302.
(10) Yang, H.; Lu, C.; Liu, Z.; Jin, H.; Che, Y.; Olmstead, M. M.; Balch, A. L. *J. Am. Chem. Soc.* **2008**, *130*, 17296–17300.
(11) Mercado, B. Q.; Jiang, A.; Yang, H.; Wang, Z.; Jin, H.; Liu, Z.; Olmstead, M. M.; Balch, A. L. *Angew. Chem., Int. Ed.* **2009**, *48*, 9114–9116.
(12) Stevenson, S.; Rice, G.; Glass, T.; Harich, K.; Cromer, F.; Jordan, M. R.; Craft, J.; Hadju, E.; Bible, R.; Olmstead, M. M.; Maitra, K.; Fisher, A. J.; Balch, A. L.; Dorn, H. C. *Nature* **1999**, *401*, 55–57.
(13) Chaur, M. N.; Melin, F.; Ashby, J.; Elliott, B.; Kumbhar, A.; Rao, A. M.; Echegoyen, L. *Chem.—Eur. J.* **2008**, *14*, 8213–8219.
(14) Valencia, R.; Rodriguez-Fortea, A.; Poblet, J. M. *Chem. Commun.* **2007**, 4161–4163.
(15) Yang, T.; Zhao, X. A.; Nagase, S. *Phys. Chem. Chem. Phys.* **2011**, *13*, 5034–5037.
(16) Kurihara, H.; Lu, X.; Iiduka, Y.; Mizorog, N.; Slanina, Z.; Tsuchiya, T.; Akasaka, T.; Nagase, S. *J. Am. Chem. Soc.* **2011**, *133*, 2382–2385.
(17) Crystal data for D_5(450)-La_2@C_{100}·2Ni^{II}(OEP)·2(toluene): $C_{186}H_{104}La_2N_8Ni_2$, M = 2846.01; black parallelepiped, 0.13 mm × 0.09 mm × 0.08 mm; λ = 0.74490 Å, Advanced Light Source, beamline 11.3.1; monoclinic, space group *Pbca* (No. 61); a = 24.6803(7) Å, b = 19.0086(6) Å, c = 24.8761(8) Å; T = 100(2) K; U = 11670.3(6) Å^3; Z = 4; 292 557 reflections measured, 47 472 unique (R_{int} = 0.073) that were used in all calculations; Bruker SMART Apex II; $2\theta_{max}$ = 101.7°; min/max transmission = 0.841/0.898 (multiscan absorption correction applied); Patterson and difference Fourier methods solution; full-matrix least-squares based on F^2 (SHELXS97 and SHELXL97); Final $wR(F_2)$ = 0.2411 (all data), conventional R_1 = 0.0726 computed for 2267 parameters with 6768 restraints.
(18) (a) Rodriguez-Fortea, A.; Alegret, N.; Balch, A. L.; Poblet, J. M. *Nature Chem.* **2010**, *2*, 955–961. (b) Rodriguez-Fortea, A.; Balch, A. L.; Poblet, J. M. *Chem. Soc. Rev.* **2011**, *40*, 3551–3563.
(19) Ishitsuka, M. O.; Sano, S.; Enoki, H.; Sato, S.; Nikawa, H.; Tsuchiya, T.; Slanina, Z.; Mizorogi, N.; Liu, M. T. H.; Akasaka, T.; Nagase, S. *J. Am. Chem. Soc.* **2011**, *133*, 7128–7134.